*Journal of the European Ceramic Society* **5** (1989) 173–182

# Electrical Properties and Defect Structure of Barium Metatitanate within the p-Type Regime

J. Nowotny* & M. Rekas

Max-Planck-Institute for Solid State Research, 7000 Stuttgart 80, FRG

(Received 8 May 1989; revised version received 4 September 1989; accepted 13 September 1989)

**Abstract**

*Both electrical conductivity ($\sigma$) and thermopower ($\alpha$) data are reported within the p-type regime for undoped $BaTiO_3$ in the temperature range 1268–1418 K. The experimental data are considered against several models of the $BaTiO_3$ defect structure. It has been documented that both electron holes and electrons participate in the conduction process. It has been argued that electron holes may be generated as a result of different processes such as ionization of acceptor-type impurities and intrinsic defects. In considerations of the defect models it has been assumed that within the p-type regime the concentration of oxygen vacancies is negligibly low and predominant defects are both cation vacancies and acceptor-type extrinsic defects. Thus the determined intrinsic equilibrium constant is the following function of $p_{O_2}$ and temperature:*

$$K = [V''_{Ba}][V''''_{Ti}][h^{\cdot}]^6 p_{O_2}^{-3/2} = 3{\cdot}1 \times 10^{-29} \exp\left(-\frac{3{\cdot}65\,[eV]}{kT}\right)$$

*Die elektrische Leitfähigkeit ($\sigma$) und die Thermokraft ($\alpha$) sind in Temperaturbereich zwischen 1268 und 1418 K für nicht dotiertes $BaTiO_3$ als p-Leitungstyp veröffentlicht. Die experimentellen Daten sprechen gegen verschiedene Modelle über die Defektstruktur von $BaTiO_3$. Es wurde berichtet, daß sowohl Elektronenleerstellen als auch Elektronen am Leitungsprozeß teilnehmen. Die Argumentation war, daß die Elektronenleerstellen durch zwei verschiedene Prozesse, wie der Ionisation von akzeptorartigen Verunreinigungen und dem elektronischen Eigengleichgewicht hervorgerufen werden. In Anbetracht der Defektmodelle wurde angenommen, daß im p-Leitungsbereich die Konzentration der Sauerstoffleerstellen vernachlässigbar gering ist und die vorherrschenden Defekte entweder die Kationenleerstellen oder die extrinsischen akzeptorartigen Störstellen sind. Die so bestimmte Eigengleichgewichtskonstante beschreibt die folgende Gleichung in Abhängigkeit von $p_{O_2}$ und Temperatur:*

$$K = [V''_{Ba}][V''''_{Ti}][h^{\cdot}]^6 p_{O_2}^{-3/2} = 3{\cdot}1 \times 10^{-29} \exp\left(-\frac{3{\cdot}65\,[eV]}{kT}\right)$$

*On présente des données sur la conductivité électrique ($\sigma$) et la puissance thermique ($\alpha$) en régime de type p d'un $BaTiO_3$ non-dopé pour des températures allant de 1268 à 1418 K. Les données expérimentales sont confrontées à plusieurs modèles sur la structure à défauts du $BaTiO_3$. On a documenté le fait que les trous et les électrons participent tous deux au processus de conduction. On a avancé que les trous électroniques pourraient être produits par différents processus comme l'ionisation d'impurités de type accepteur et l'équilibre électronique intrinsèque. Lors de l'examen des modèles de défauts, on a supposé, en régime de type p, que la concentration des vacances oxygène est négligeable et que les défauts prédominants sont les vacances cationiques et les défauts extrinsèques de type accepteur. Ainsi déterminée, la constante d'équilibre intrinsèque est la fonction suivante de $p_{O_2}$ et de la température:*

$$K = [V''_{Ba}][V''''_{Ti}][h^{\cdot}]^6 p_{O_2}^{3/2} = 3{\cdot}1 \times 10^{-29} \exp\left(-\frac{3{\cdot}65\,[eV]}{kT}\right)$$

## 1 Introduction

Barium metatitanate ($BaTiO_3$) exhibits both the n-type and the p-type regimes at elevated temperatures. Figure 1 illustrates the dependence between

* Present address: Australian Nuclear Science & Technology Organisation, Lucas Heights Research Laboratories, Menai, New South Wales 2234, Australia.



*Journal of the European Ceramic Society* 0955-2219/90/$3.50 

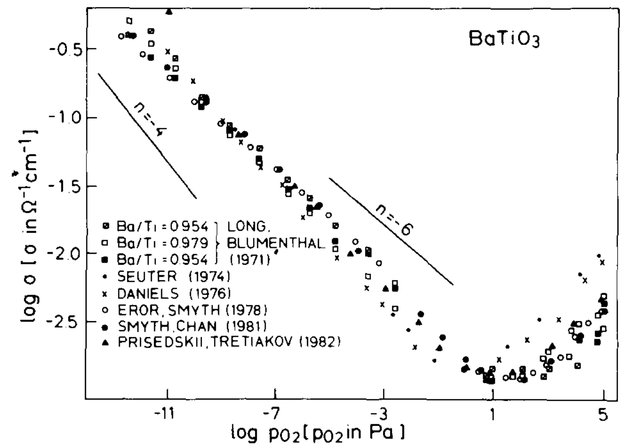


**Fig. 1.** The plot of log $\sigma$ versus log $p_{O_2}$ at 1273 K according to literature reports.[1-6]

the electrical conductivity and oxygen partial pressure at 1273 K involving experimental data taken from various reports.[1-6] As can be seen there is a good agreement between the experimental data within the n-type regime. Consequently, the defect structure in this regime can be discussed against a relatively well-defined experimental background. On the other hand, the p-type regime exhibits a substantial scatter of experimental data within a very narrow range of $p_{O_2}$. This is the reason that little is known on the defect structure of $BaTiO_3$ within this regime.

There are several defect models which have been postulated for $BaTiO_3$ within the p-type regime. The first approach is essentially based on both Ba and Ti vacancies as predominant defects.[1] The second model involves an assumption that electrical properties are controlled by acceptor-type extrinsic defects such as impurities and unintentionally introduced elements.[2] Also the intrinsic nonstoichiometry in the cation sublattices involving an excess of Ba or Ti ($[Ba] \neq [Ti]$) has also been considered.[1] Finally, the formation of oxygen vacancies was also taken into account.[5]

As can be seen from literature reports the considerations on the defect structure of $BaTiO_3$ have been limited mainly to the n-type regime, while little is known about the p-type regime for which several conflicting defect models have been postulated.[1-5]

The objective of this work was to perform studies on the electrical properties of $BaTiO_3$ within its p-type regime and to reanalyze its defect structure within the p-type regime where the Schottky disorder is predominant. Both electrical conductivity and thermopower measurements will be performed at elevated temperatures and under controlled oxygen activity. The combination of these two methods is especially useful in the determination of the defect structure of nonstoichiometric compounds. Experimental data will be analyzed against existing models in the literature.

## 2 Experimental

### 2.1 Sample preparation

Samples were prepared by coprecipitation of Ba and TiO oxalates. The oxalates were filtered, and washed with water until $Cl^-$ ions were no longer detected. The precipitate was then dried at 380 K. The calcination of precipitates was performed at 873 K and then at 1173 K for 2 h. Finally, the calcinate was annealed at 1673 K for 3 h in air in order to perform

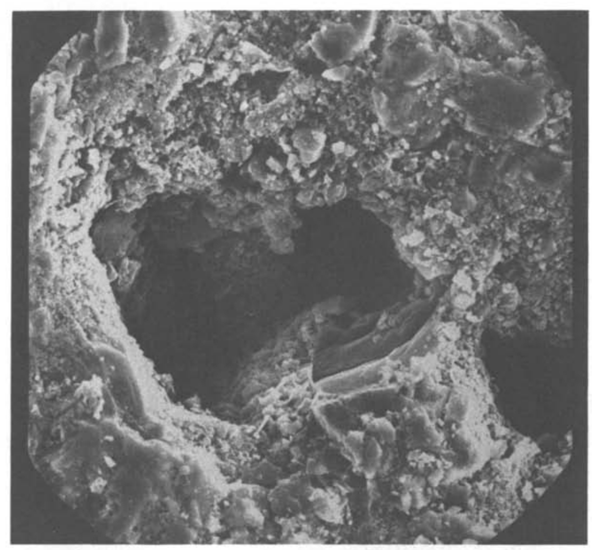

(a)

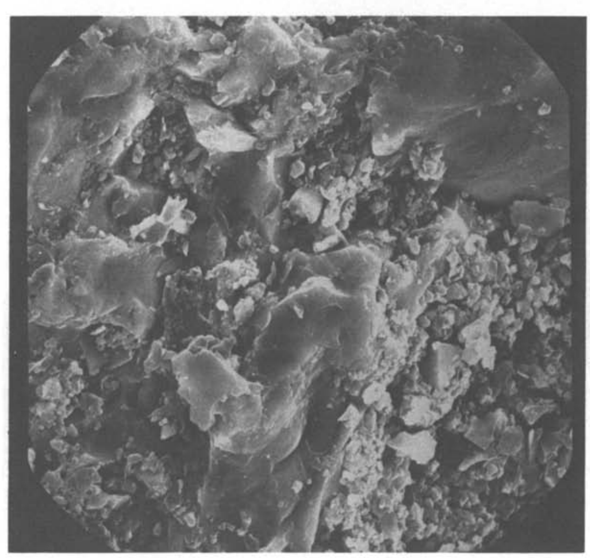

(b)

**Fig. 2.** SEM micrographs of a sintered $BaTiO_3$ specimen. Original magnification: (a) ×2000, (b) ×5000.

the synthesis of the oxide system. Rectangular pellets (4 × 4 × 20 mm) were formed under the pressure 500 MPa. The pellets were sintered at 1773 K for 2 h in air. Figure 2 shows the SEM micrograph of the specimen. As can be seen from the micrograph the grain size varies between 0·2 and 4 $\mu$m.

## 2.2 Experimental procedure

The sample holder for the determination of both thermopower (Seebeck coefficient) and electrical conductivity have been described elsewhere in detail.[7] The sample was placed between two Pt electrodes which are attached to microheaters at both sides (Fig. 3). The microheaters served to

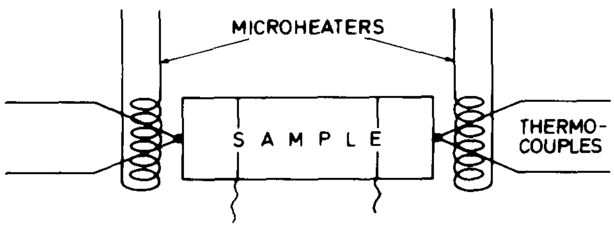


**Fig. 3.** The sample holder for measurements of the thermopower and electrical conductivity.

impose the required temperature gradient across the sample. The Pt electrodes were used to measure the thermopower as well as to impose an external voltage for the determination of the electrical conductivity. Two Pt wires wrapped around the sample were used as two internal probes for the measurements of the electrical conductivity.

Absolute values of the thermopower ($\alpha$) of the studied oxide material were determined assuming the following temperature dependence of $\alpha$ for Pt:[8]

$$\alpha_{Pt} = -2{\cdot}63 - 0{\cdot}0145T[\mu V\,K^{-1}] \qquad (1)$$

The required oxygen partial pressure was imposed by an appropriate $Ar/O_2$ gas mixture flowing over the sample. The measured values of thermopower ($\alpha$) and electrical conductivity ($\sigma$) were taken after the equilibrium in the studied system was reached, i.e. after both $\alpha$ and $\sigma$ remained stable for several hours. The oxygen activity in the gas phase was determined by a zirconia oxygen gage installed at the gas exit from the reaction chamber.

# 3 Results and Discussion

Figures 4 and 5 illustrate the dependence of both $\alpha$ and $\sigma$ as a function of $\log p_{O_2}$ between 25 and $10^5$ Pa. As seen there is a linear dependence of $\log \sigma$ versus $\log p_{O_2}$ in the range $10^3$ to $10^5$ Pa, which indicates a

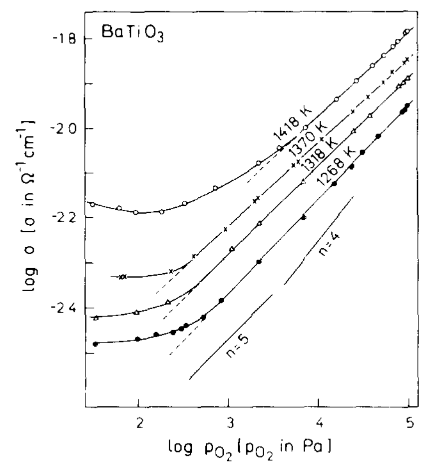


**Fig. 4.** Plots of $\log \sigma$ as a function of $\log p_{O_2}$.

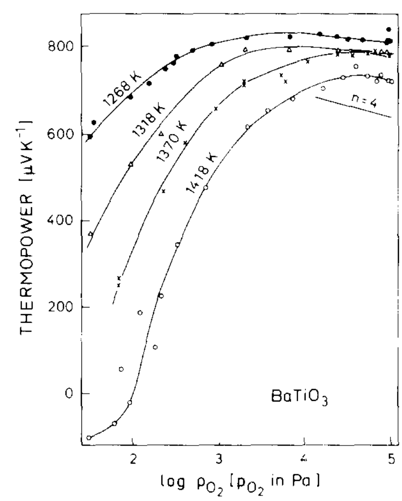


**Fig. 5.** Plots of thermopower as a function of $\log p_{O_2}$.

p-type character of the conduction. On the other hand, the lack of linearity in the $\alpha$ versus $\log p_{O_2}$ dependence indicates that electrons may make a substantial contribution to the conduction process and resulting thermopower data. As it has been reported for CoO[9] and $SrTiO_3$,[10] minor type electronic carriers usually have larger effect on $\alpha$ than on $\sigma$. This effect is consistent with the following expressions for both $\sigma$ and $\alpha$:

$$\sigma = q(\mu_e[e'] + \mu_h[h^{\bullet}]) \qquad (2)$$

$$\alpha = \frac{\mu_e[e']\alpha_e + \mu_h[h^{\bullet}]\alpha_h}{\mu_e[e'] + \mu_h[h^{\bullet}]} \qquad (3)$$

where

$$\alpha_{e,h} = \pm \frac{k}{q}\left(\ln \frac{N_{e,h}}{[e,h]} + A_{e,h}\right) \qquad (4)$$

$q$ is the elementary charge, $\mu_e$ and $\mu_h$ are the mobility term of electrons and electron holes, respectively, $\alpha_e$ and $\alpha_h$ is the thermopower component corresponding to electrons and electron holes, respectively,

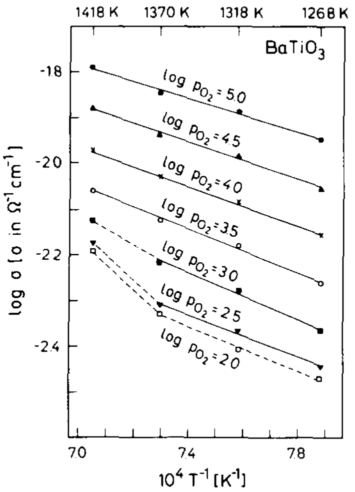


**Fig. 6.** Arrhenius-type plots of electrical conductivity.

$k$ is the Boltzmann constant, $N_e$ and $N_h$ is the density of states of donor and acceptor centres, respectively, and $A_e$ and $A_h$ is the kinetics term for electrons and electron holes, respectively. As can be seen from Fig. 5 the thermopower exhibits a linear relationship which is limited to a small $p_{O_2}$ range close to $10^5$ Pa. At 1418 K the thermopower exhibits a change of sign from '+' at $p_{O_2} = 10^2$ Pa to '−' below this value. This effect corresponds to the minimum of $\sigma$ in Fig. 4.

Figure 6 illustrates the Arrhenius-type plots of $\sigma$. As can be seen, the experimental data fulfil the linearity above $10^3$ Pa. Thus the determined activation energy values ($E_\sigma$) are plotted versus $\log p_{O_2}$ (Fig. 7). The monotonous decrease of $E_\sigma$ with $p_{O_2}$ suggests that more than one source of the formation of electron holes should be taken into account. This suggestion may find its confirmation in the variation of the oxygen pressure exponent of electrical conductivity ($1/n$) versus oxide composition. The

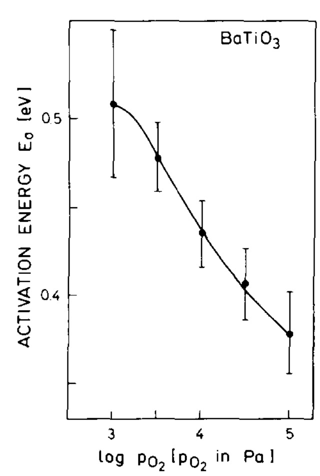


**Fig. 7.** The plot of the activation energy as a function of $\log p_{O_2}$.

**Table 1.** The reciprocal of electrical conductivity oxygen exponent (eqn (5))

| $n$ | *log of $p_{O_2}$ range ($p_{O_2}$ in Pa)* | *Temperature (K)* |
|---|---|---|
| $4{\cdot}81 \pm 0{\cdot}045$ | 2·7–5 | 1 268 |
| $5{\cdot}12 \pm 0{\cdot}062$ | 2·6–5 | 1 318 |
| $5{\cdot}41 \pm 0{\cdot}041$ | 2·6–5 | 1 370 |
| $5{\cdot}40 \pm 0{\cdot}080$ | 3·6–5 | 1 418 |

reciprocal of the exponent can be expressed as follows:

$$n = \left( \frac{\partial \log \sigma}{\partial \log p_{O_2}} \right)_T^{-1} \tag{5}$$

The parameters $n$ are listed in Table 1.

From general considerations of the $BaTiO_3$ defect structure[11] the following defect reactions may be taken into account:

$$O_O \leftrightarrows 1/2O_2 + V_O^{\bullet\bullet} + 2e' \tag{6}$$

$$3/2O_2 \leftrightarrows 3O_O + V_{Ba}'' + V_{Ti}'''' + 6h^{\bullet} \tag{7}$$

$$A_M \leftrightarrows A_M' + h^{\bullet} \tag{8}$$

$$\text{zero} \leftrightarrows h^{\bullet} + e' \tag{9}$$

where $A_M$ is an acceptor-type cation impurity and M denotes the Ba or the Ti site. Application of the mass action law to eqns (6), (7) and (9) results in the following equilibrium constants:

$$K_1 = [V_O^{\bullet\bullet}][e']^2 p_{O_2}^{1/2} \tag{10}$$

$$K_2 = [V_{Ba}''][V_{Ti}''''][h^{\bullet}]^6 p_{O_2}^{-3/2} \tag{11}$$

$$K_i = [e'][h^{\bullet}] \tag{12}$$

Because of a very high value of the dielectric constant and a low concentration of defects in $BaTiO_3$ the considerations of equilibria (10)–(12) are based on an assumption that concentrations are equal to activities. As can be seen from eqns (6)–(9) the lattice electroneutrality condition requires that:

$$[A'] + [e'] + 2[V_{Ba}''] + 4[V_{Ti}''''] = 2[V_O^{\bullet\bullet}] + [h^{\bullet}] \tag{13}$$

In eqn (13) the term [A′] denotes an effective concentration of acceptors. Assuming that acceptor-type impurities are predominant then the component [A′] denotes the difference between the entire concentration of acceptors and donors regarding their individual valency. The formation of defect complexes should also be taken into account.

Thus, from eqns (10)–(12):

$$(2K_1 K_i^{-2} p_{O_2}^{-1/2})[h^{\bullet}]^5 + [h^{\bullet}]^4 - [A'][h^{\bullet}]^3 - K_i[h^{\bullet}]^2 - 6K_2^{1/2} p_{O_2}^{3/4} = 0 \tag{14}$$

For the condition (14) the following two assumptions may be considered:

(a) the concentration of cation vacancies is negligibly low, and
(b) the concentration of oxygen vacancies within the p-type regime is negligibly low.

In the first case eqn (14) results in the following form:

$$n_h = \left(\frac{\partial \ln [h^{\cdot}]}{\partial \ln p_{O_2}}\right)_T^{-1} = 6 - \frac{2[A']/[h^{\cdot}] - 4}{[e']/[h^{\cdot}] + [A']/[h^{\cdot}] - 1} \quad (15)$$

In the second case the following is obtained:

$$n_h = \frac{8}{3} + \frac{4}{3}\frac{[A']/[h^{\cdot}] - 2}{[e']/[h^{\cdot}] + [A']/[h^{\cdot}] - 1} \quad (16)$$

Figures 8(a) and (b) illustrate the dependences of $n_h$ on the $[A']/[h^{\cdot}]$ ratio according to eqns (15) and (16), respectively. As can be seen in case (a), $n_h$ decreases with $[A']/[h^{\cdot}]$ to minus infinity ($-\infty$) within

$$0 \le [A']/[h^{\cdot}] \le 1 - [e']/[h^{\cdot}]$$

while in the range

$$[A']/[h^{\cdot}] > 1 - [e']/[h^{\cdot}]$$

$n_h$ decreases to 4. Then the electroneutrality condition requires that:

$$[A'] = 2[2V_O^{\cdot\cdot}] \quad (17)$$

Since with the increasing temperature the term $[A']/[h']$ decreases, therefore, within $[A']/[h^{\cdot}] > 1 - [e']/[h^{\cdot}]$ the parameter $n_h$ increases between 4 and infinity. On the other hand, when $[A']/[h^{\cdot}] < 1 - [e']/[h^{\cdot}]$ the parameters $n_h$ increases between $-\infty$ and 2.

In the second case—(b)—changes in the parameter $n_h$ are as follows:

(1) $n_h$ increases to $+\infty$ when $0 \le [A']/[h^{\cdot}] < 1 - [e']/[h^{\cdot}]$, and
(2) $n_h$ increases between $-\infty$ and 4 when $[A']/[h^{\cdot}] > 1 - [e']/[h^{\cdot}]$.

With the increasing temperature $n_h$ initially decreases between 4 and $-\infty$ and then between $+\infty$ and 5·3.

Thus the determined values of $n_h$ are the same as the oxygen pressure exponent resulting from $\sigma$ (eqn (5)) when the $[e']/[h^{\cdot}]$ ratio is low. Both $n_h$ and $n_\sigma$ may substantially differ when $[e']/[h^{\cdot}]$ assumes higher values. For evaluating the difference between $n_\sigma$ and $n_x$, eqn (2) may be expressed as follows:

$$\sigma = q(\mu_e[e'] + \mu_h(h^{\cdot}]) = q\mu_h\left([h^{\cdot}] + \frac{bK_i}{[h^{\cdot}]}\right) \quad (18)$$

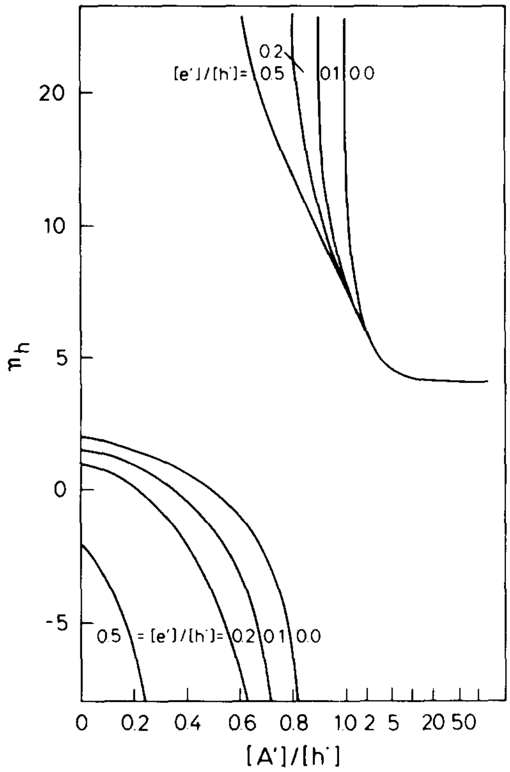


(a)

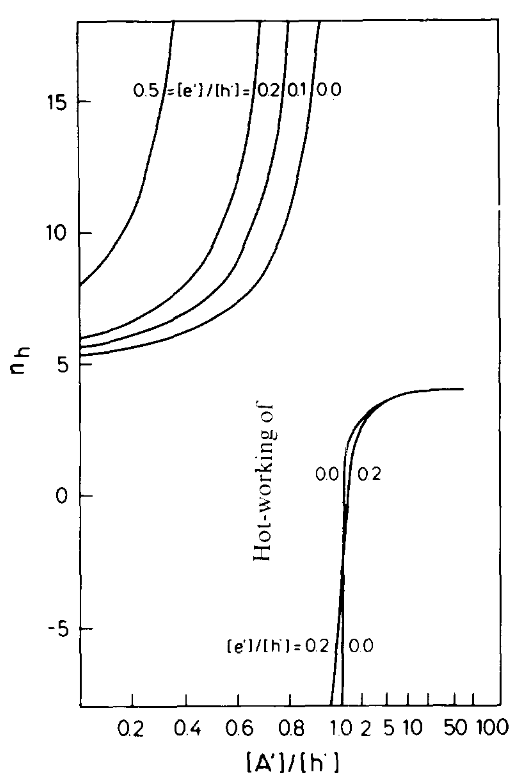


(b)

**Fig. 8.** Plots of $n_h$ as a function of the $[A']/[h^{\cdot}]$ ratio determined assuming (a) negligibly low concentrations of cation vacancies and (b) negligibly low concentrations of oxygen vacancies within the p-type region.

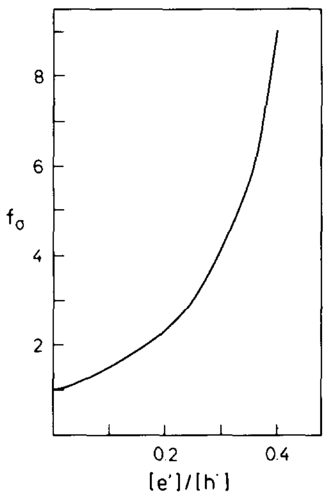


**Fig. 9.** The plot of the parameter $f_\sigma$ as a function of the [e′]/[h˙] ratio (for $b = 2$).

where $b = \mu_e/\mu_h$. For $BaTiO_3$ the parameter $b$ is close to 2.[5,12] Therefore, eqn (5) assumes the form:

$$n = n_h \frac{1 + b[e']/[h^\cdot]}{1 - b[e']/[h^\cdot]} = n_h f_\sigma \qquad (19)$$

Figure 9 illustrates the dependence of $f_\sigma$ as a function of the [e′]/[h˙] ratio at $b = 2$. Accordingly, the comparative analysis of both above considered cases (a) and (b) against experimental data of $n$ (Table 1) does not allow one to decide which of these cases is valid for $BaTiO_3$. More precise criterion of their validity can be obtained by an analysis based on absolute values of $\sigma$ as a function of its components in eqn (2).

### 3.1 Case (a)

The following lattice electroneutrality condition can be considered for the p-type regime:[5]

$$[h^\cdot] + 2[V_O^{\cdot\cdot}] = [A'] \qquad (20)$$

Taking into account eqns (10) and (12) and also that

$$\sigma = q\mu_h[h^\cdot] \qquad (21)$$

then

$$\sigma = -\frac{2\sigma^2}{K_p p_{O_2}^{1/2}} c + [A']/c \qquad (22)$$

where

$$c = 1/(q\mu_h) \qquad (23)$$

$$K_p = K_i^2/K_1 \qquad (24)$$

Figures 10(a) and (b) illustrate the dependence of $\sigma$ as

$$\sigma = f\left(\frac{2\sigma^2}{K_p p_{O_2}^{1/2}}\right) \qquad (25)$$

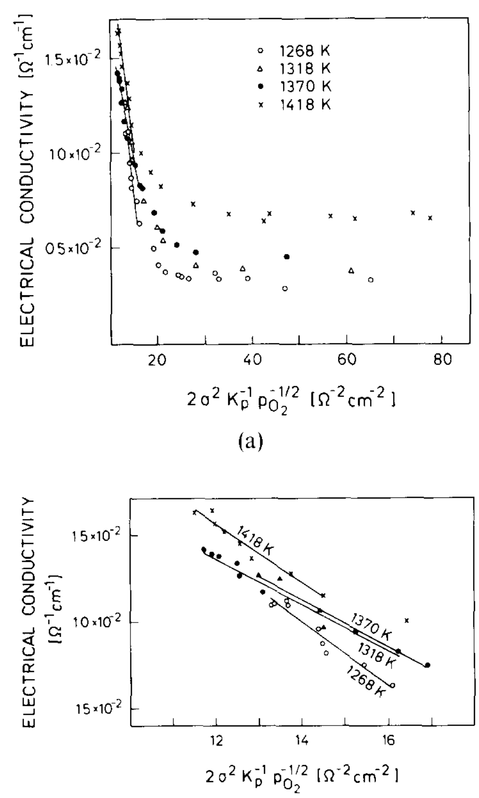


**Fig. 10.** Plots of the electrical conductivity versus the product $2\sigma^2 K_p^{-1} p_{O_2}^{-1/2}$. (a) The entire range, (b) a fragment of the dependence corresponding to high $p_{O_2}$.

where the constant $K_p$ assumes[13]

$$K_p = 2.63 \times 10^{-4} \exp\left(-\frac{-88.6\,[\mathrm{kJ} \times \mathrm{mol}^{-1}]}{RT}\right) \qquad (26)$$

As can be seen eqn (25) fulfils the linearity only within a limited part of experimental data corresponding to high $p_{O_2}$. Thus determined values of $c$ and [A′] are listed in Table 2. Assuming that $\mu_h = 0.075\ \mathrm{cm^2\,V^{-1}\,s^{-1}}$,[13] eqn (2) gives

$$c_{calc} = 5.48 \times 10^{-3}\ \Omega\mathrm{cm}$$

This value is about three times higher than the average $\bar{c}$ value from Table 2 corresponding to a single crystal. For a polycrystalline specimen used in

**Table 2.** Parameters $c$ and [A′] in eqn (22)

| *Temperature (K)* | *c (Ω cm)* | *[A′] (ppm)* |
|---|---|---|
| 1 268 | 0.001 84 ± 0.000 27 | 66 ± 5 |
| 1 318 | 0.001 36 ± 0.000 20 | 41 ± 4 |
| 1 370 | 0.001 33 ± 0.000 10 | 39 ± 2 |
| 1 418 | 0.001 67 ± 0.001 30 | 60 ± 3 |

the present studies the values of both $\bar{c}$ and $c_{calc}$ may differ as a result of intergranular contacts:

$$\frac{\bar{c}}{c_{calc}} = \frac{\sigma_{cr}}{\sigma_{pol}} > 1 \tag{27}$$

where $\sigma_{cr}$ and $\sigma_{pol}$ denote $\sigma$ for single crystalline and polycrystalline sample, respectively. The obtained results do not agree with this expectation. As seen from Table 2 the average level of acceptor-type impurities is about 50 ppm. These values are somewhat lower than the concentrations estimated by Chan *et al.*[5] However, in contrast to their expectation, here, a tendency of increasing the concentration of so-called 'active acceptors' with temperature is not observed. According to Chan *et al.*[5] this tendency is related to the formation of defect complexes $(A'V_O^{\bullet\bullet})$ at lower temperatures. What is surprising, however, that despite the different parameters, $n_\sigma$, determined by Chan *et al.* on the one hand and in the present work on the other, the determined concentration of impurities is comparable. This apparent conflict will be analyzed below in more detail.

### 3.2 Case (b)

Assuming cation vacancies as predominant defects within the entire p-type regime the condition (13) may be written in the form:

$$6[V_{Ba}''] + [A'] = [h^{\bullet}] \tag{28}$$

where

$$[V_{Ba}''] = [V_{Ti}'''']$$

Therefore

$$\sigma = \frac{6K_2^{1/2}}{c^4\sigma^3} p_{O_2}^{3/4} + \frac{[A']}{c} \tag{29}$$

Figure 11 illustrates the dependence of $\sigma$ as a function of $p_{O_2}^{3/4}/\sigma^3$. As seen there is a better agreement of eqn (29) with experimental data than

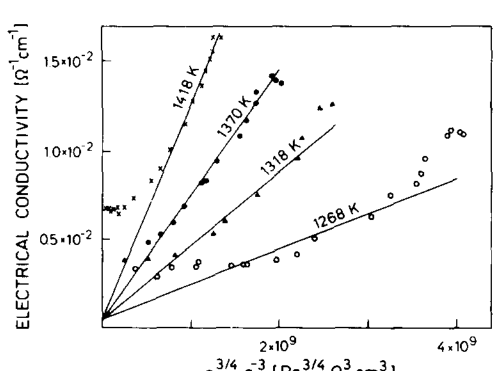


**Fig. 11.** Plots of electrical conductivity versus the product $p_{O_2}^{3/4}\sigma^{-3}$.

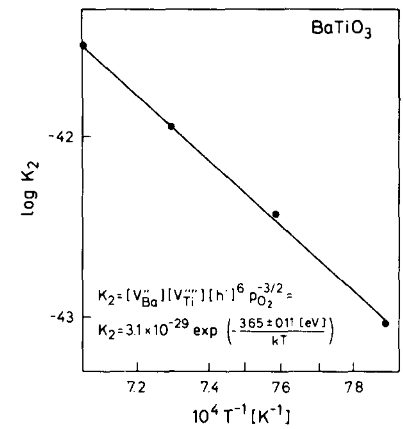


**Fig. 12.** Arrhenius plot of the equilibrium contant $K_2$.

was observed for case (a). Assuming the same value of $c$ ($5{\cdot}48 \times 10^{-3}\,\Omega\,cm$) the following is obtained:

$$[A'] = (2{\cdot}5 \pm 1{\cdot}0) \quad [ppm]$$

Thus the determined equilibrium constant $K_2$ assumes the following expression (Fig. 12):

$$K_2 = [V_{Ba}''][V_{Ti}''''][h^{\bullet}]^6 p_{O_2}^{-3/2} = 3{\cdot}1 \times 10^{-29} \exp\left(-\frac{3{\cdot}65 \pm 0{\cdot}11\,[eV]}{kT}\right) \tag{30}$$

## 4 Considerations on Equilibration Kinetics

In the discussion of the Schottky-type defect structure the most important point arises about the kinetics of equilibration of different defect processes. In other words, the relationship (30) may be interpreted as an equilibrium constant only if the measured electrical parameters of both $\sigma$ and $\alpha$, which served for the determination of the equilibrium constant $K_2$, correspond to the equilibrium state of the studied gas/solid system. Therefore, it seems of interest to consider the available data on diffusion in $BaTiO_3$. Also the criteria assumed in this work for the definition of equilibrium state will be analyzed.

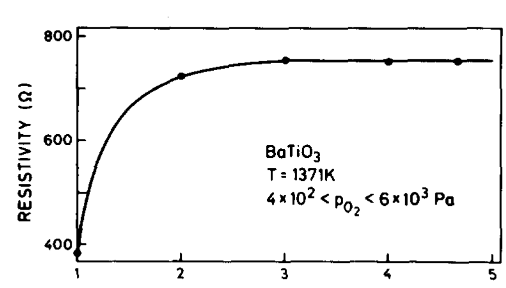


**Fig. 13.** The equilibration conductivity curve for $BaTiO_3$ at 1371 K.

Figure 13 illustrates a typical kinetic curve obtained in this work, in the form of the resistivity versus logarithm of time. The curve illustrates the rate of the equilibration. As can be seen from the kinetic data, the equilibrium state at 1371 K is reached after about 3 h.

Diffusion data for $BaTiO_4$ were reported by Wernicke[14] for both oxygen and barium vacancies:

$$D_{V_O} = 5{\cdot}7 \times 10^3 \exp(-2.05\,[\mathrm{eV}]/kT) \quad [\mathrm{cm}^2\,\mathrm{s}^{-1}] \tag{31}$$

$$D_{V_{Ba}} = 6{\cdot}8 \times 10^{-2} \exp(-2{\cdot}76\,[\mathrm{eV}]/kT) \quad [\mathrm{cm}^2\,\mathrm{s}^{-1}] \tag{32}$$

Using these values equilibration times for the smallest ($d = 0{\cdot}2\ \mu$m) and the largest (4 $\mu$m) grain size in the present specimens have been calculated. For evaluation of the equilibration time the chemical diffusion coefficient ($\tilde{D}$) was used, which is the following function of diffusion coefficient of defects ($D_d$) and their effective charge:

$$\tilde{D} = (1 + z)D_d \tag{33}$$

where $z$ is an absolute value of charge of diffusing defects. Appropriate values of the equilibration time at different temperatures applied in the present studies involving the measurements of both $\sigma$ and $\alpha$ as well as at the temperature of preparation are illustrated in Table 3.

Wernicke[14] has interpreted his diffusion values assuming that the equilibration process is rate controlled by Ba vacancies. He has ignored the existence of Ti vacancies. According to Lewis *et al.*[15] the activation energy of diffusion for Ti vacancies is much higher. However, since the pre-exponential factor is not known it is impossible to ignore the participation of these defects in the equilibration process. Accordingly, the diffusion data reported by Wernicke[14] for Ba vacancies may also be considered in terms of Ti vacancies as rate controlling the equilibration kinetics. This alternative interpretation of Wernicke's diffusion data is based on the following equilibrium:

$$\mathrm{zero} \leftrightarrows 3V_O^{\bullet\bullet} + V_{Ba}'' + V_{Ti}'''' \tag{34}$$

Corresponding penetration times at this assumption are listed in Table 3 in parentheses. As seen the equilibration time resulting from Fig. 13 (3 h at 1370 K) exhibits a good agreement with the penetration time resulting from Table 3. Similar agreement has been found at other temperatures.

Since, on the one hand, Ti vacancies have been generally assumed for $BaTiO_3$ and, on the other hand, their diffusion is presumably lower than that of Ba vacancies, it is assumed that the diffusion data reported by Wernicke may be interpreted in terms of Ti vacancies rather than Ba vacancies. Based on these diffusion data and equilibration kinetic data from this report it is concluded that the parameter $K_2$ may be interpreted as the equilibrium constant of the intrinsic disorder.

## 5 General Considerations on the Intrinsic and Extrinsic Disorder in $BaTiO_3$

The intrinsic defect model proposed in this work is in an obvious conflict with the extrinsic model reported by Long and Blumenthal[2] and then confirmed by Chan *et al.*[5,13] In contrast to Chan *et al.*,[5] who have reported that the $p_{O_2}$ dependence within the p-type regime is exactly $+1/4$, the parameter $n_\alpha$ in the present work varies between $+4{\cdot}81$ and $+5{\cdot}4$ at 1268 and 1418 K, respectively. These conflicting reports may be considered either in terms of the purity of studied specimens or assuming that the reported electrical conductivity data do not correspond to the equilibrium state. Assuming that the data of both Chan *et al.*[5] and those of the present work are taken in equilibrium the difference may

**Table 3.** Diffusion time for $BaTiO_3$ at different grain sizes ($d$) after Wernicke[14]

| *Number* | *Temperature (K)* | *zero* $\leftrightarrows V_O^{\bullet\bullet} + 1/2O_2 + 2e'$ | | *zero* $\leftrightarrows 3V_O^{\bullet\bullet} + V_{Ba}'' + V_{Ti}''''$ | |
|---|---|---|---|---|---|
| | | *d* = 0·2 μm (μs) | *d* = 4 μm (ms) | *d* = 0·2 μm (s) | *d* = 4 μm (h) |
| 1 | 1 268 | 270 | 110 | 108 (108)[a] | 20 (12)[a] |
| 2 | 1 318 | 1·6 | 0·7 | 72 (43) | 8 (5) |
| 3 | 1 370 | 0·8 | 0·3 | 28 (17) | 3 (2) |
| 4 | 1 418 | 0·5 | 0·2 | 13 (8) | 1·5 (0·83) |
| 5 | 1 773 | 0·2 | 0·07 | 4 (2) | 0·42 (0·25) |

[a] Values in parentheses correspond to diffusion of Ti vacancies as the rate controlling step of the equlibration kinetics.

indicate much higher concentration of acceptor-type impurities in the specimen studied by Chan *et al.* Comparable concentration values reported in both cases apparently result in different models assumed for their determinations. It seems that exact knowledge of the impurity level based on chemical analysis could supply a decisive argument on the validity of the two models. Unfortunately, the level of impurities required to be determined is below the detectability limit.

As an argument confirming their model Chan *et al.*[5] report the determination of the enthalpies of oxidation and reduction which is exactly equal to twice the band gap. This relationship has been interpreted as being in obvious contradiction with any intrinsic disorder. This implies, as they claim, that the production of vacancies by any process other than reduction is zero. This argumentation, however, assumes that the lattice electroneutrality condition based *a priori* on the extrinsic disorder described by eqn (6) and the following relations:

$$V_0^{\cdot\cdot} + 1/2O_2 \leftrightarrows O_0 + 2h^{\cdot} \tag{35}$$

$$2[V_0^{\cdot\cdot}] = [A'] + [e'] \tag{36}$$

In other words their 'confirmation' of the extrinsic disorder is valid only when the condition (eqn (36)) is assumed as valid. Consequently, Chan *et al.*,[5] 'confirm' what they initially assume as valid. It seems that their consideration can only be understood as a confirmation of generally accepted relationship:

$$[e'][h^{\cdot}] = K\exp\left(-\frac{E_g}{kT}\right) \tag{37}$$

where $E_g$ is the band gap.

Taking into account that the sum of equilibria (6) and (35) is described by the intrinsic electronic disorder:

$$\text{zero} \leftrightarrows e' + h^{\cdot} \tag{38}$$

one may conclude that Chan *et al.*[5] have confirmed the relationship (37) but this confirmation cannot be considered for any reason as an argument either against the intrinsic disorder or confirming the extrinsic disorder.

A certain weakness of the extrinsic model involves the temperature dependence of so called 'active' acceptors on temperature reported by Chan *et al.*[5] They argue that this dependence may indicate the formation of defect complexes. The present authors did not find this argument consistent with a high value of the dielectric constant of $BaTiO_3$.

## 6 Conclusions

A narrow $p_{O_2}$ range of the p-type regime results in certain difficulties in the studies of the $BaTiO_3$ defect model in this regime. According to the present experimental data and literature reports on defect models it has been documented that both Ba and Ti vacancies are predominant defects in $BaTiO_3$ within experimental conditions under study. A knowledge of the level of impurities and their individiual effect on electrical properties of undoped (but not pure) $BaTiO_3$ is of a fundamental importance for a precise analysis of the defect structure. The effective concentration of acceptors may have a substantial effect on electrical parameters already at the level of several tens of ppm.

Based on equilibration kinetic data obtained in this work and the reported diffusion data one may conclude that experimental conditions applied in the present studies correspond to the equilibrium of the Schottky-type disorder, confirmed in this work.

It seems that detailed analysis of the impurity spectrum on the level of several ppm is required to bring more conclusive argument concerning conflicting defect models reported in the literature.

## References


1. Seuter, A. M. J. H., Defect chemistry and electrical transport properties of barium titanate. *Philips Res. Repts Suppl.*, No. 3 (1974) 1–84.
2. Long, S. A. & Blumenthal, R. N., Ti-rich nonstoichiometric $BaTiO_3$: I. High-temperature electrical conductivity measurements. *J. Am. Ceram. Soc.*, **54**(10) (1971) 515–19.
3. Daniels, J. & Härdtl, K. H., Defect chemistry and electrical conductivity of doped barium titanate ceramics. Part I. Electrical conductivity at high temperatures of donor doped barium titanate ceramics. *Philips Res. Repts*, **31** (1976) 489–504.
4. Eror, N. G. & Smyth, D. M., Nonstoichiometric disorder in single-crystalline $BaTiO_3$ at elevated temperatures. *J. Solid State Chem.*, **24**(3–4) (1978) 235–44.
5. Chan, N. H., Sharma, R. K. & Smyth, D. M., Nonstoichiometry in undoped $BaTiO_3$. *J. Am. Ceram. Soc.*, **64**(9) (1981) 556–62.
6. Prisedskii, V. V. & Tret'yakov, Yu.D., Chemistry of point defects in an oxide ferroelectric. *Izv. AN SSSR, Neorg. Mater.*, **18**(12) (1982) 1926–38.
7. Nowotny, J. & Rekas, M., Seebeck effect of undoped and Cr-doped NiO. *Solid State Ionics*, **12** (1984) 253–61.
8. Landolt-Börnstein, In *Numerical Data and Functional Relationships in Science and Technology*, New Series, ed. O. Madelung, K. H. Hellwege & J. L. Olsen. Springer-Verlag, Berlin, III 15 b 1985, pp. 48–104.
9. Nowotny, J. & Rekas, M., Defect structure of CoO. II. The Debye-Hückel model. *J. Am. Ceram. Soc.*, **72**(7) (1989) 1207–14.
10. Choi, G. M. & Tuller, H. L., Defect structure and electrical properties of single-crystal $Ba_{0.03}Sr_{0.97}TiO_3$. *J. Am. Ceram. Soc.*, **71**(4) (1988) 201–5.
11. Nowotny, J. & Rekas, M., Defect chemistry of $BaTiO_3$. *J. Europ. Ceram. Soc.*, (in press).

12. Choi, G. M., Tuller, H. L. & Goldschmidt, D., Electronic transport behaviour in single-crystalline $Ba_{0.03}Sr_{0.97}TiO_3$. *Phys. Rev. B*, **34**(10) (1986) 6972–9.
13. Chan, N. H., Sharma, R. K. & Smyth, D. M., Nonstoichiometry in acceptor-doped $BaTiO_3$. *J. Am. Ceram. Soc.*, **65**(3) (1982) 167–70.
14. Wernicke, R., Defect chemistry and electrical conductivity of doped barium titanate ceramics. Part IV. The kinetics of equilibrium restoration in barium titanate ceramics. *Philips Research Reports*, **31** (1976) 526–43.
15. Lewis, G. V., Catlow, C. R. A. & Casselton, R. E. W., PTCR effect in $BaTiO_3$. *J. Am. Ceram. Soc.*, **68**(10) (1985) 555–8.